

# Effect of noble gas ion pre-irradiation on deuterium retention in tungsten

L Cheng<sup>1</sup>, Z H Zhao<sup>2</sup>, G De Temmerman<sup>3</sup>, Y Yuan<sup>1</sup>, T W Morgan<sup>4</sup>, L P Guo<sup>5</sup>, B Wang<sup>6</sup>, Y Zhang<sup>1</sup>, B Y Wang<sup>7</sup>, P Zhang<sup>7</sup>, X Z Cao<sup>7</sup> and G H Lu<sup>1\*</sup>

<sup>1</sup> School of Physics and Nuclear Energy Engineering, Beihang University, Beijing 100191, China

<sup>2</sup> China Institute of Atomic Energy, Beijing 102413, China

<sup>3</sup> ITER Organization, Route de Vinon sur Verdon, CS90 046, 13067 St Paul Lez Durance Cedex, France

<sup>4</sup> FOM Institute DIFFER, Dutch Institute For Fundamental Energy Research, Association EURATOM-FOM, Trilateral Euregio Cluster, Eindhoven, the Netherlands

<sup>5</sup> School of Physics and Technology, Wuhan University, Wuhan 430072, China

<sup>6</sup> College of Materials Science and Engineering, Beijing University of Technology, Beijing 100124, China

<sup>7</sup> Institute of High Energy Physics in Chinese Academy of Sciences, Beijing 100049, China

Email: LGH@buaa.edu.cn

**Abstract.** Impurity seeding of noble gases is an effective way of decreasing the heat loads onto the divertor targets in fusion devices. To investigate effect of noble gases on deuterium retention, tungsten targets have been implanted by different noble gas ions and subsequently exposed to deuterium plasma. Irradiation induced defects and deuterium retention in tungsten targets have been characterized by positron annihilation Doppler broadening and thermal desorption spectroscopy. Similar defect distributions are observed in tungsten irradiated by neon and argon, while it is comparatively low in the case of helium. The influence of helium pre-irradiation on deuterium trapping is found to be small based on the desorption spectrum compared with that of the pristine one. Neon and argon pre-irradiation leads to an enhancement of deuterium trapping during plasma exposure. The influence on deuterium retention is found to be argon > neon > helium when comparing at a similar crystal damage level.

Keywords: Noble gas, tungsten, deuterium retention

PACS: 52.40.Hf

## 1. Introduction

Tungsten (W) is chosen as the divertor armour material in ITER [1] and considered as the main candidate for plasma facing materials (PFMs) in future fusion reactors [2]. W divertor armour is bombarded by hydrogen isotopes and various impurities during operations. Impurities such as helium (He) are generated by fusion reactions, and neon (Ne) and/or argon (Ar) can be injected into the divertor plasma to decrease the heat loads onto the divertor targets as demonstrated in JET [3] and ASDEX Upgrade [4]. The irradiation of these noble gas impurities modifies the physical state of W in the near-surface region which affects the hydrogen (H) isotopes transport. The effect of He irradiation on H retention has been noted in earlier literatures and reviewed in [5,6]. Pre-irradiation with a low He incident energy of 20 eV prior to deuterium (D) plasma exposure results in a reduction of D retention [7]. He occupation of D-trap sites can lead to a decrease in the effective number of trap sites available for D atoms and thus resulting in a reduced D retention. However, when the incident energy is far beyond the damage threshold, enhanced D retention is observed due to significant crystal damage [8,9]. There is little work done to investigate the effect of Ne and Ar on D retention in W. In our previous work, we have explored D retention in W pre-irradiated by Ne plasma with 20 eV incident energy in Pilot-PSI [10]. A reduced D retention due to Ne pre-irradiation is found at different exposure temperatures. Theoretically the clustering behavior of He, Ne and Ar in W is demonstrated to be quite different in [11], showing a stronger self-trapping tendency of Ne and Ar compared to He. In this study, D retention is studied in W targets which are pre-implanted by various noble gas ions (He, Ne and Ar) and subsequently exposed to high-flux D plasma in Pilot-PSI. The same W damage level was created in each case and the role of crystal damage by different noble gases on D retention was evaluated.

## 2. Experimental details

Recrystallized polycrystalline tungsten targets (>99.95 wt.% purity) with an average grain size of 55  $\mu\text{m}$  from Advanced Technology and Materials Co., Ltd. China were mechanically polished to a mirror-like finish. After polishing the targets were annealed at 1273 K for one hour at a background pressure of  $5 \times 10^{-4}$  Pa. Each target was a 10 mm  $\times$  10 mm square of 1.0 mm in thickness.

The noble gas ion irradiation was performed at the Accelerator Laboratory in Wuhan University by using a J59200-200kV ion implanter [12]. The beam is uniformly distributed over a square of 20 mm  $\times$  20 mm, permitting the simultaneous irradiation of two targets. The surface temperature was kept at 473 K during irradiation. The irradiation parameters are shown in table 1. SRIM calculations [13] were made to predict the irradiation damage with a displacement threshold energy of 90 eV in the mode of full damage cascades. The calculation results of damage distribution and implantation ion concentration distribution are shown in figure 1. Various irradiation energies and fluences were used for different ion species to obtain similar damage profiles. All the damage profiles extend approximately 0.1  $\mu\text{m}$  below the surface and show a maximum of  $\sim 0.33$  dpa at 20-40 nm.

The pre-irradiated W targets were then exposed to D plasma in the linear plasma generator Pilot-PSI located at the FOM-Institute DIFFER which is described in details in [14]. The plasma is produced by a cascaded arc source and confined by an axial magnetic field of 0.4 T. The plasma

beam has a Gaussian profile with a peak electron density of  $\sim 4 \times 10^{20} \text{ m}^{-3}$  and a full width half maximum of  $\sim 10 \text{ mm}$  as measured using Thomson scattering. The electron temperature of D plasmas is  $\sim 1 \text{ eV}$ . This yields a D ion flux of  $\sim 1.4 \times 10^{24} \text{ m}^{-2}\text{s}^{-1}$ . The incident ion energy is about 40 eV which is dominated by the -40 V negative target bias as the plasma potential is relatively small (a few V). The plasma beam center is aligned with the target center. The temperature profile of the target surface is measured by an infrared camera with an emissivity set to 0.05. The surface temperature radial profile is similar to that of the electron density. The reported surface temperatures as well as the ion fluxes and fluences are taken at the center of the plasma beam. In this study the W targets are exposed to a fixed D fluence of  $1.0 \times 10^{26} \text{ m}^{-2}$  at 520 K.

Before and after the D plasma exposure, positron annihilation Doppler broadening (PADB) was used to monitor the formation of vacancy-type defects [15,16]. In the annihilation reaction between an electron and a positron, two gammas, each with an average energy of 511 keV are generated. The momentum distribution of the electron-positron pair results in the Doppler broadening of the 511 keV annihilation gamma energy spectrum. S parameter, which describes the width of the Doppler broadened 511 keV annihilation peak, is commonly used to monitor the presence of the defects. The PADB measurements were performed with slow positrons in the Institute of High Energy Physics in Chinese Academy of Sciences [17]. Positrons were injected into the targets with various kinetic energies in the range of 0.5 keV to 20.5 keV. The corresponding positron average range is from 0.6 to 250 nm in W. During PADB measurement the gamma spectra from 504.2 to 517.8 keV were counted. The S parameter is determined by the area ratio from 510.2 keV to 511.8 keV in the central spectra which makes the S parameter sensitive to annihilations with low momentum valence electrons. This implies that S parameter is relatively high for materials with defects such as dislocations, mono-vacancies and vacancy clusters. The diameter of the positron beam is  $\sim 8 \text{ mm}$  and the beam is directed towards the target center.

Finally the targets were analyzed by thermal desorption spectroscopy (TDS). The targets were linearly heated up to 1273 K at 1 K/s. D<sub>2</sub> (mass 4) and HD (mass 3) were monitored by a quadrupole mass spectrometer. The absolute sensitivity of the mass 2 and 4 signals was determined by a calibrated leak, while that of mass 3 is assumed to be the average of the sensitivities for masses 2 and 4. When calculating the total D retention, D atoms from HD and D<sub>2</sub> are taken into account.

### 3. Results and discussion

The PADB results measured after different noble gas ions irradiation (hereafter referred as He-W, Ne-W, Ar-W) are shown in figure 2(a). Elevated S parameters are observed in all irradiated targets after ion irradiation, with Ar-W showing the highest value. The curves show a similar peak distribution as indicated in the SRIM calculation, but with a peak position closer to the surface and an affected depth deeper than 170 nm. The main damage products are expected to be vacancies or small vacancy clusters [18]. Other defects with open volume such as dislocations may also contribute to elevated S parameters but are not well separated from vacancies or vacancy clusters in this PADB setup. The discussion of damage products is thus mainly based on vacancies or vacancy clusters. The mechanism of defect production depends on the recoil energy absorbed by the target W atoms [19]. Separated vacancy and interstitial pairs as a result of replacement collision sequences (RCS) are expected in case of low recoil energy of hundreds eV

in case of He irradiation, while in cases of Ne and Ar due to the high recoil energy of thousands eV vacancy clusters and even dislocation loop containing several vacancies are produced. The main deviation in damage profile from SRIM calculation is observed in the He-W case, where S parameter is lower than that of Ne-W and Ar-W. Several factors may result in this deviation. Initially the collision cascade induced by ion irradiation leads to the formation of displaced atoms in a certain region, the radius of which determined primarily by the ion mass [20]. Subsequently the collision cascade becomes a thermal spike where displaced atoms recombine with vacancies. As He atom is much lighter than Ne and Ar, He irradiation results in a smaller affected zone where more recombination happens with respect to Ne and Ar irradiation. Though it is predicted by SRIM that a similar damage level (that is, the amount of displaced atoms) is generated by He, Ne and Ar, the recombination (not considered in the SRIM code) leads to less vacancy formation and thus to a lower damage efficiency in the He case. In addition, the He fluence is almost two orders of magnitude higher than Ne or Ar fluence to achieve the same damage level, resulting in a high He concentration in the target as shown in figure 1(b). The occupation of vacancies by He is expected [21] at such a high fluence. The He occupation repels positrons from entering the vacancies and results in a reduced S parameter [22]. Considering the damage efficiency and He occupation during irradiation, both are ascribed to a reduced S parameter.

The ion-implanted and pristine targets exposed to D plasma in Pilot-PSI were measured by PADB (hereafter referred as He-D-W, Ne-D-W, Ar-D-W and D-W) as shown in figure 2(b). The D-W target shows an enhanced S parameter while an opposite trend of decreasing S parameter after D plasma is observed in the ion-implanted targets. The S parameter of He-W after D exposure falls to the same level as that of D-W. The S parameter of Ne-D-W is again slightly lower than that of Ar-D-W, and both decrease to a similar level with a higher absolute value than that of D-W. Note that the evolution of S parameter after D plasma exposure is dependent on both the generation of defect such as vacancies [23] and the trapping of D in vacancies [24]. W exposed to a high flux D plasma usually shows an increased S parameter due to the generation of plasma-induced damage [24]. While in the case of noble gas pre-irradiation, pre-existing vacancies serve as trapping sites for the impinging D atoms. The trapped D atoms in vacancies play a similar role as He to decrease S parameter as mentioned in the previous paragraph.

The D<sub>2</sub> desorption spectra of the ion-implanted and pristine targets are shown in figure 3 and the total retention in each targets is included in the last column of table 1. For the D-W, He-D-W and Ne-D-W the desorption profile is characterized by two main release peaks at 500-550 K and 600-800 K, while in the case of Ar-D-W a distinct release peak at ~800 K appears. The desorption spectrum of He-D-W is rather similar to that of D-W and shows a D retention reduction of 12.4%. In the cases of Ne and Ar pre-irradiation a strong desorption peak at 700 K – 800 K is observed, which results in an increased total D retention. Compared with D-W the total D retention in the two cases is increased by 55.7% and 97.9%, respectively. The desorption peaks at 700 K and 800 K are assigned to trapping sites such as plasma-induced damage (e.g. vacancy-clusters or bubbles) and chemisorption on the void inner surface, respectively [25–27]. These types of defects are seldom produced in D-W and He-D-W and more readily produced in Ne-D-W and Ar-D-W in the TDS spectra. The observation well agrees with the PADB results where Ne-D-W and Ar-D-W demonstrate higher S parameters. A simple estimation is done to evaluate the D trapping level of Ne/Ar irradiation under certain Ne/Ar fluence. Assuming the 700 K – 800 K peak intensities (subtracted by the peak intensity in D-W) are triggered by Ne or Ar pre-irradiation, the D trapping level of Ne is 17.3 D/Ne and that of Ar is 598.9 D/Ar.

Though the damage level of He, Ne and Ar is controlled to be at the same level of 0.33 dpa, their effect on D retention is different. He pre-irradiation at this He fluence has relatively small effect on the subsequent D retention. It does not enhance the D plasma-induced damage and even partly mitigates the D retention. The result is partly comparable to that in [7] where He plasma pre-irradiation leads to a reduced D retention and a similar shape of D desorption profile. The result is explained by the He occupation of D-trap sites which leads to a decrease in the effective number of trap sites available for D atoms and thus a reduced D retention. Though He ion energy in this research differs quite a lot from that (20 eV) in [7], He occupation of the vacancy or vacancy cluster at the He fluence is expected to play a similar role on D retention. Vacancies generated during He pre-irradiation are filled by He, thus no more D is trapped by the vacancies during subsequent D plasma exposure. In case of Ne and Ar, both are found to enhance D retention strongly. Both D desorption and PADB results indicate Ar pre-irradiation leads to the highest W-matrix damage and D retention. It should be noted that the ion pre-irradiation energy in our experiment is beyond the expected ion energy in the divertor, and thus less D retention with high desorption temperatures is expected as less irradiation-induced damage is produced.

#### 4. Conclusion

In the present experiments, effects of various noble gases pre-irradiation on D retention in W have been investigated. Although the damage level is predicted to be the same for all the ions, the PADB measurements show that Ne and Ar are able to produce more vacancy-type defects than He. Moreover, Ne and Ar pre-irradiation leads to a strong D trapping at high desorption temperatures of 700 K – 800 K and high total retention while He pre-irradiation has little influence on D retention. The different effect of noble gas ion pre-irradiation relies on both the crystal damage efficiency by noble gas and the noble gas occupation of defects.

#### Acknowledgement

This work was supported by National Magnetic Confinement Fusion Science Program of China under Grant 2013GB109003 and the National Nature Science Foundation of China under contract No.51401012. G H Lu acknowledges the support from the China National Funds for Distinguished Young Scientists under Grant 51325103. This work was partially financially supported by the Nederlandse Organisatie voor Wetenschappelijk Onderzoek (NWO).

#### Reference

- [1] R A Pitts *et al* 55th APS Meeting, Denver, CO, USA, Paper WE1.00001
- [2] Philipps V 2011 *J. Nucl. Mater.* **415** S2–9
- [3] Rapp J *et al* 2004 *Nucl. Fusion* **44** 312–9
- [4] Schweinzer J *et al* 2011 *Nucl. Fusion* **51** 113003
- [5] Ueda Y *et al* 2013 *J. Nucl. Mater.* **442** S267–72
- [6] Baldwin M J *et al* 2011 *Nucl. Fusion* **51** 103021
- [7] Nishijima D *et al* 2005 *J. Nucl. Mater.* **337-339** 927–31
- [8] Hino T *et al* 1998 *Fusion Eng. Des.* **39-40** 227–33
- [9] Iwakiri H *et al* 2002 *J. Nucl. Mater.* **307-311** 135–8

- [10] Cheng L *et al* 2015 *J. Nucl. Mater.* **463** 1025–8
- [11] Tamura T *et al* 2014 *Model. Simul. Mater. Sci. Eng.* **22** 015002
- [12] Guo L P *et al* 2008 *Nucl. Instruments Methods Phys. Res. Sect. A Accel. Spectrometers, Detect. Assoc. Equip.* **586** 143–7
- [13] Ziegler J F *et al* 2010 *Nucl. Instrum. Methods Phys. Res. B* **268** 1818–23
- [14] De Temmerman G *et al* 2011 *Nucl. Fusion* **51** 073008
- [15] Schut H 1990 A variable energy positron beam facility with applications in materials science *Thesis* Delft University of Technology, Delft
- [16] Van Veen A 1990 *J. trace microprobe Tech.* **8** 1–29
- [17] Bao-Yi W *et al* 2010 *Chinese Phys. C* **32** 156–9
- [18] Debelle a *et al* 2007 *J. Nucl. Mater.* **362** 181–8
- [19] Diaz de la Rubia T 1996 *Nucl. Instruments Methods Phys. Res. Sect. B Beam Interact. with Mater. Atoms* **120** 19–26
- [20] Morehead F F *et al* 1970 *Radiat. Eff.* **6** 27–32
- [21] Lhuillier P E *et al* 2011 *J. Nucl. Mater.* **416** 13–7
- [22] Anon A Van Veen, I de Vries, D Segers, G J Rozing, in: P C Jam, R M Singru, K P Gopinathan (Eds.), *Positron Annihilation*, World Scientific Publ. Co., Singapore, 1985, p. 543
- [23] Wright G M, *et al* 2010 *Nucl. Fusion* **50** 075006
- [24] Xu H Y *et al* 2014 *J. Nucl. Mater.* **447** 22–7
- [25] Van Veen a *et al* 1998 *J. Nucl. Mater.* **155-157** 1113–7
- [26] 't Hoen M H J *et al* 2014 *Nucl. Fusion* **54** 083014
- [27] Ogorodnikova O *et al* 2003 *J. Nucl. Mater.* **313-316** 469–77

Captions:

**Table 1.** Parameters of noble gas ion irradiation at 473 K. The total D retention determined by TDS after D plasma exposure is also included.

**Figure 1.** SRIM results of (a) damage distribution and (b) implantation ion concentration distribution for tungsten irradiated by He, Ne and Ar ions with different incident energy. The He concentration is divided by 10 to match the plot scale.

**Figure 2.** (a) The S parameter versus the average positron irradiation depth in the W for ion pre-irradiated W and pristine W. (b) The S parameter versus the average positron irradiation depth in the W for W exposed to D plasma. Results of the pristine W and W exposed to only D plasma are included in both figures for comparison.

**Figure 3.** TDS D<sub>2</sub> desorption profiles for noble gas pre-irradiated W targets exposed to D plasma at 520 K. The heating rate was 1 K/s for all targets.

**Table 1.**

Noble gas ion pre-irradiation	Energy (keV)	Ion flux ( $\times 10^{16} \text{ m}^{-2} \text{ s}^{-1}$ )	Fluence ( $\times 10^{18} \text{ m}^{-2}$ )	Total Retention ( $\times 10^{19} \text{ D m}^{-2}$ )
-	-	-	-	8.54
He	20	9.03	112	7.48
Ne	80	5.16	4.87	13.3
Ar	140	0.97	1.87	16.9

**Figure 1.**

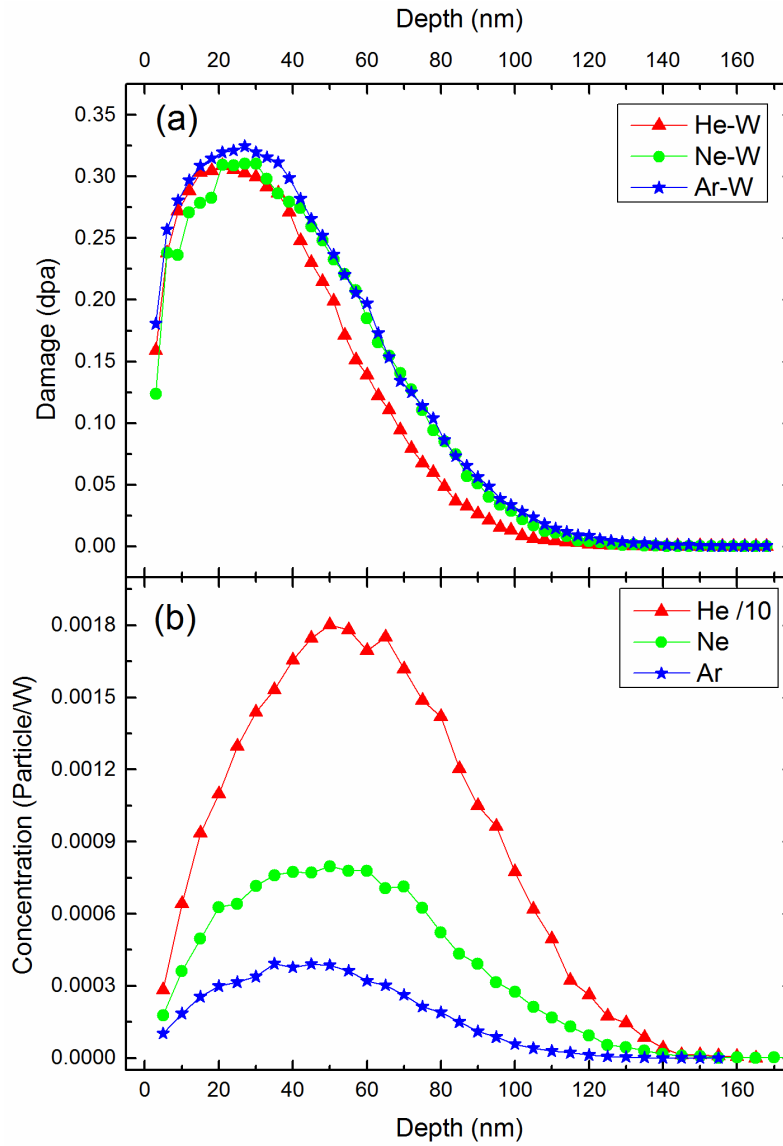


**Figure 2.**



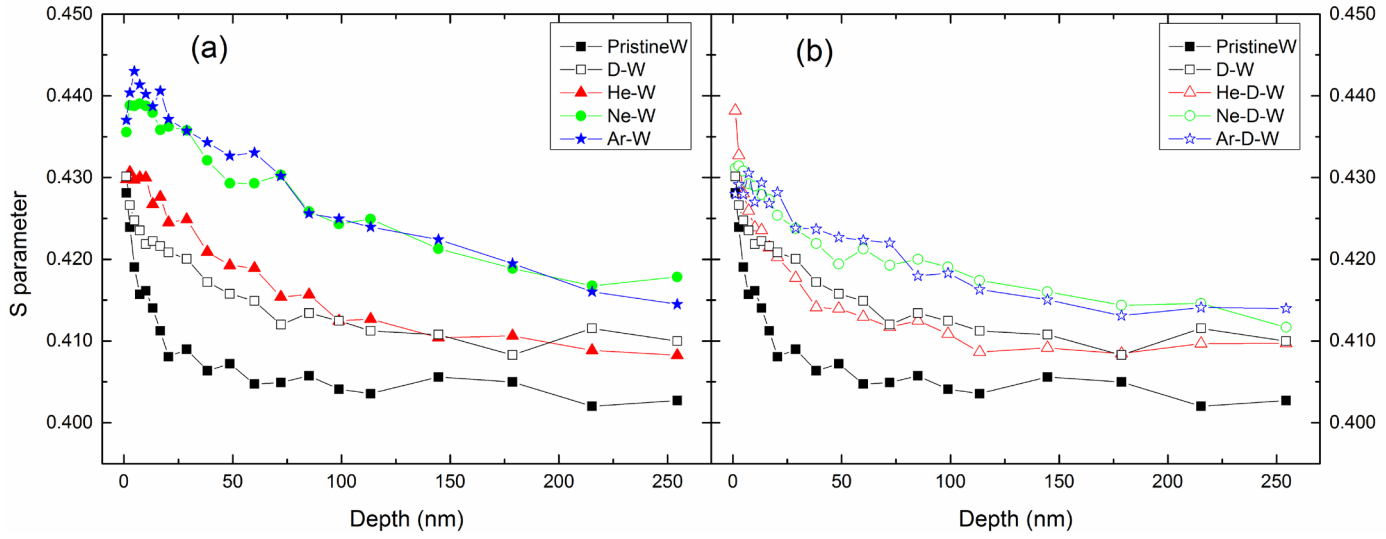


Figure 3.

